COBEM 2023 27TH INTERNATIONAL CONGRESS OF MECHANICAL ENGENEERING

ABCM Brazilian Society of Mechanical Sciences and Engineering
27th ABCM International Congress of Mechanical Engineering
December 04-08, 2023, Florianópolis-SC, Brazil

COB-2023-2115

INVESTIGATION OF THE CAVITATION PHENOMENON EFFECT IN THE MECHANICAL AND METALLURGICAL PROPERTIES OF THE ROTOR OF THE FRANCIS TYPE TURBINE MADE OF STAINLESS STEEL ASTM A743 GR CF20

Carlos Eduardo da Silva Moreira
Lecino Caldeira
Matheus José Cunha de Oliveira
Paula Graciele Silvestre
Instituto Federal do Sudeste de Minas Gerais, IF Sudeste MG, Juiz de Fora, MG
cesm18@hotmail.com
lecino.caldeira@ifsudestemg.edu.br
matheus.oliveira@ifsudestemg.edu.br
paula.lucas@ifsudestemg.edu.br

Cristian Pohl Meinhardt
Universidade Federal do Pampa, UNIPAMPA, Alegrete, RS
cristianmeinhardt@unipampa.edu.br

Abstract. *Industrial equipment such as hydraulic turbines are susceptible to cavitation wear. This generates a progressive loss of material on the rotor surface, reducing the turbine service. Such loss is caused by the collapse of vapor bubbles formed in a liquid at critical pressure and temperature. It is known that knowing the condition of the internal structure of the material, that is, its microstructure, is of fundamental importance to verify the existence of some correlation between the microstructure and the phenomenon of cavitation. For research purposes, the focus of this work is a Francis model rotor, with a diameter of 740 mm, widely used in Hydroelectric Power Plants (HPPs) to generate up to 750 MW. Material of construction is ASTM A743 GR CF20 austenitic stainless steel, a foundry alloy containing iron-chromium-nickel for general applications requiring corrosion and cavitation resistance. The characterization of the sample taken in the region of the rotor affected by cavitation was performed through microstructural analysis, macrography, energy dispersive X ray spectroscopy (EDX) test and hardness test. According to the results obtained, it was verified that the analyzed material presents porosities and cracks under the influence of tensile stresses, which can facilitate the occurrence of the phenomenon of cavitation on the rotor surface. In microscopy, dendritic structures were observed in the region of the Fused Zone (FZ), grain growth and intergranular corrosion (sensitization) in the region of the Heat Affected Zone (HAZ), characterized by the precipitation of chromium carbide in the grain boundaries. The analysis highlights the formation of cracks from the FZ towards the HAZ and the formation of cavities in the Base Metal (BM) region. The analyzed crack presents intragranular aspects in the HAZ region and are attributed to sensitization and to the state of tensile stress, characteristic of the rotor in operation. The sample also presents singularities (circular shape) in the BM region. These singularities were formed by the cavitation phenomenon, and can assist the formation of cracks, which were also observed in the MB region, taking into account the effect of stress concentration caused by the singularities and adding to the state of tensile stress, characteristic of the operation. In the EDX test, percentages of chromium and nickel were found within the range of the chemical composition of austenitic stainless steel CF20, 18% to 21% of chromium and 8% to 11% of nickel, in accordance with the ASTM A743 standards.*

Keywords: *cavitation, francis rotor, cast stainless steel, ASTM A743 GR CF20*

1. INTRODUCTION

The Francis turbine is the most used turbine model in hydroelectric power plants. In this type of turbine, the water enters through a helical tube with reduced cross-sectional area. In this helical tube, the water experiences a decrease in pressure in the suction region, that is, at the exit of the turbined water and an increase in the rotor speed through the blades. This turbine model is used for small and large hydroelectric power plants with rotor diameters ranging from 0.5 m to 12 m due to its great versatility and efficiency (Marinho, 2015). The main wear mechanisms of Francis turbines are erosion, cavitation and abrasion. Erosion and cavitation occurs on the rotor, wear rings and moving vanes of the distributor, while abrasion wear occurs more frequently on the rotor shaft, as seen in Figure 1.

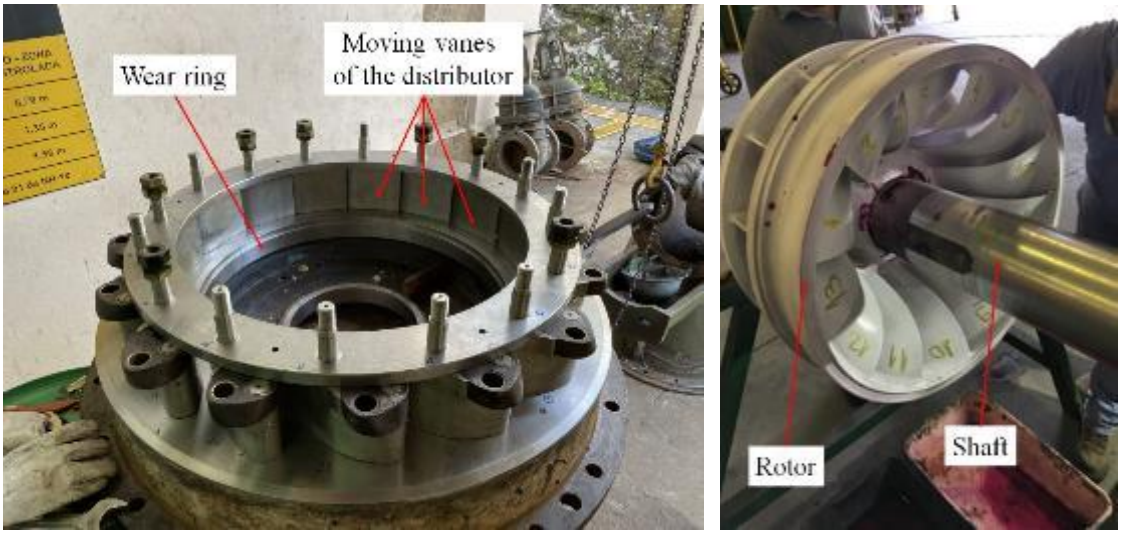

Figure 1. Main elements that make up the Francis model turbine set.

Cavitation wear is the most recurrent due to the operational characteristic of the rotor. Cavitation occurs on the rotor surfaces, cover plates and guided vanes, removing parts of the material. Cavitation wear is so severe that the rotor can lose balance in some cases (imbalance) and eventually cause serious problems, such as unit shutdown. Furthermore, the efficiency of the turbines drops significantly, which leads to a significant drop in revenue for power generation companies (Horta et al., 1999). Cavitation is defined as the gradual loss of material from a solid surface, due to the collapse of bubbles that form in a liquid under critical pressure and temperature. The fluid evaporates during movement due to the reduction in water vapor pressure, generating bubbles. Those bubbles formed in the low pressure flow are carried to areas of high pressure. Then the bubbles implode generating wear on the surface of the Francis rotor (Fedumenti, 2010). If the bubble collapse region is close to the surface, successive implosions can generate shock waves. The bubble bursts during movement, so the wear has a spherical profile. The damage is caused by jets of liquid colliding with the metal surface. According to Hammitt and Heyman (1975), the number of cavitation pits per unit area increases on a logarithmic scale with fluid velocity, and the maximum rate of material loss generally varies exponentially with the relative velocity between the surface and the surface fluid. It is important to understand how materials respond to applied mechanical fatigue and how they absorb shock wave impact energy, whether through elastic deformation, plastic deformation or fracture.

It is also important to point out that one of the factors that influence the cavitation process is corrosion. When evaluating damage to worn rotors, it was observed that not all damage was caused by cavitation. The synergy between two forms of material wear results in severe degradation. Mechanical effects leading to electrochemical corrosion treatment include removal of the protective metal layer, resulting in a smaller anode area and greater removal of corrosion products. The final effect of cavitation will depend on the type of corrosion occurring in the system. Cavitation can increase the passivation capacitance of stainless steels if they have been previously exposed to thermal processes through solubilization heat treatment. On the other hand, if the steel is sensitized, the degree of intergranular corrosion is greatly increased by cavitation (Jiménez, 2014).

ASTM A743 GR CF20 steel is a cast austenitic stainless steel that presents good strength and ductility. Its chemical composition is composed of 18% to 21% of chromium, 8% to 11% of nickel, 1.5% of manganese, 2% of silicon and 0.04% of sulfur, which gives this steel sufficient corrosion and cavitation resistance. This steel also features suitable weldability and machinability. According to the ASTM A743 (2013) standard, its tensile strength is equivalent to 483 MPa and hardness value up to 163 HB. Its equivalent in the AISI standard is the AISI 302. The lower alloy content in these grades reduces corrosion resistance. The added sulfur further reduces the strength due to galvanic effects between the matrix and the manganese sulfide inclusions (Schweitzer, 1996).

Establishing the correlation between the mechanical properties and wear due to cavitation, the property of total resilience is used, which corresponds to the energy absorbed in the elastic deformation added to the energy in the plastic deformation of the material, proposed by Hammitt (1979),

$$TR = \frac{(TS)^2}{E} \tag{1}$$

where TR corresponds to the total resilience; TS corresponds to the ultimate tensile strength and E is the Young modulus. Hammitt (1979) also found a relationship in which the total resilience is directly proportional to the Brinell hardness, used as a parameter in stainless steel ASTM A743 GR CF20,

$$TR = HB^{1,8} \tag{2}$$

With this equation it is possible to correlate the Brinell hardness with the Average Depth of Penetration (ADP), where they are inversely proportional to each other. Furthermore, the average depth of penetration is also inversely proportional to the total resilience,

$$\frac{1}{ADP} = C.HB^{1,8} \tag{3}$$

Thus, it can be stated that the cavitation resistance of a material is directly proportional to its ability to absorb energy through elastic-plastic deformation, without fracturing, correlating hardness, which is a measurable property, to the material's ability to be resistant to cavitation (Jiménez, 2014). As for the relationship between cavitation wear and metallurgical properties, changes in the microstructure may occur due to the action of micro jets on the surface of the material, i.e., the longer the time required for changes in the microstructure, the greater the material's ability to resist cavitation wear. The microstructure that presents the best cavitation resistance performance is the one that presents the metastable austenitic phase (FCC), a characteristic present in the ASTM A743 GR CF20 stainless steel, and that can be transformed into a structure composed of austenite and martensite ε (HCP) and α' martensite (BCC), due to the impact of bubble implosion on this structure (Richman, 1995). This transition is characterized by the high resilience of the material. The cavitation wear resistance performance of a material with more than one phase will depend on the amount of that phase in relation to its dispersion in the matrix (Xiaojun, 2002). If the presence of this phase is thinner and more dispersed in the matrix, it increases resistance to cavitation wear, on the other hand, if the phase is thicker, it favors the propagation of cracks in the phase boundaries as a result of stress concentration.

2. MATERIALS AND METHODS

In order to investigate the influence of the cavitation phenomenon on the mechanical and metallurgical properties of the Francis rotor made of ASTM A743 GR CF 20 stainless steel, samples were taken by abrasive disc cutting from the rotor crown and blades in regions that presented wear points caused by cavitation and maintenance welding interventions, as seen in Figure 2.

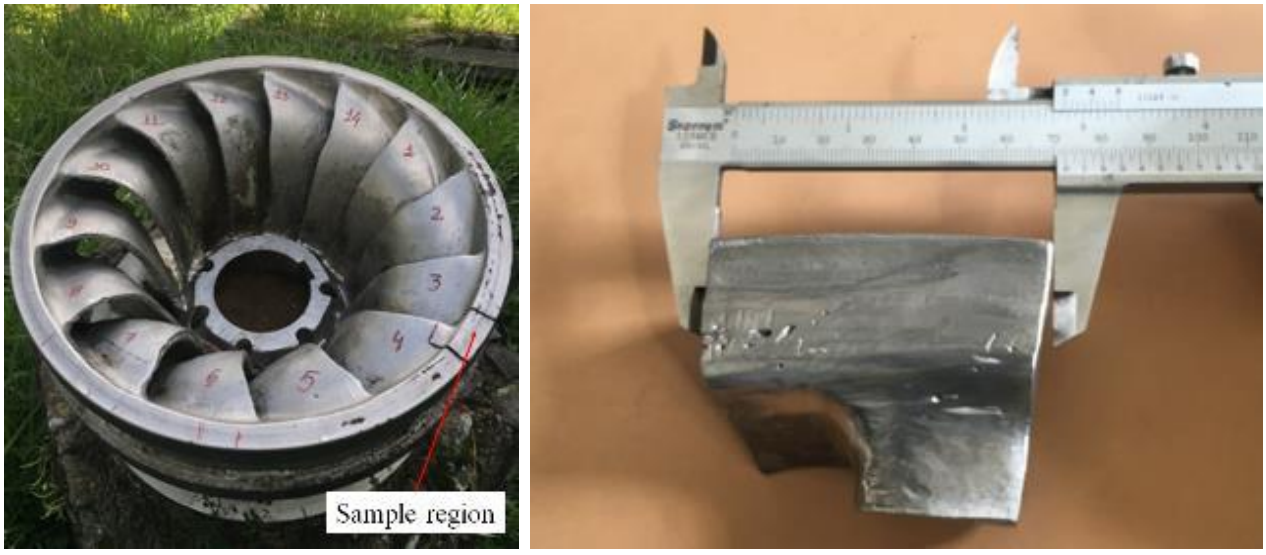

Figure 2. Francis rotor and sample extraction region for analysis, taking part of the crown and part of the rotor blade.

2.1 Metallographic analysis

Metallographic preparation was performed according to procedures recommended by the ASTM E3-11 (2017) standard. The samples were submitted to grounding on a Teclago metallographic sander, model PL02 ED and with the following sequence of sandpapers 80, 150, 320, 400, 600, 1200 and 1500 mesh. The polishing was carried out in the double polisher of the brand Arotec model PL02 in felt cloth with alumina of size 1 µm in aqueous solution. The samples also underwent an acetone wash, ultrasonic cleaning and drying in a jet of heated air, before undergoing a secondary electrolytic etching for 90 seconds at a potential of 3 volts with oxalic acid. The images of the microstructures were obtained using an Inverted Optical Microscope Olympus, model GX 51F, in interface with the Image Analysis software, with magnification of 100, 200 and 500 times, and in a Scanning Electronic Microscope Tescan Vega 3 SBU, equipped with EDS Bruker. The Energy Dispersive X-Ray Spectroscopy (EDX) test of the Shimadzu brand model EDX-7000 was also performed to check whether the chemical composition of the sample complies with the STM A743 (2013) standard.

2.2 Hardness

The polished samples were later tested in a Rockwell Durometer from Pantec, model RB, with a 1.588 mm steel ball indenter, load of 100 kgf, and 15 seconds of penetration, according to the procedures of ABNT 6508-1 (2019) standard. After the test, the hardness values obtained were converted to Brinell hardness using a standard hardness conversion table provided by ASTM E-140-12 (2019) for non-austenitic grades, recommended by the ASTM A743 standard.

3. RESULTS

In Figures 2 and 3, the micrographs taken on samples of the blade and crown of the Francis rotor in regions affected by cavitation can be seen.

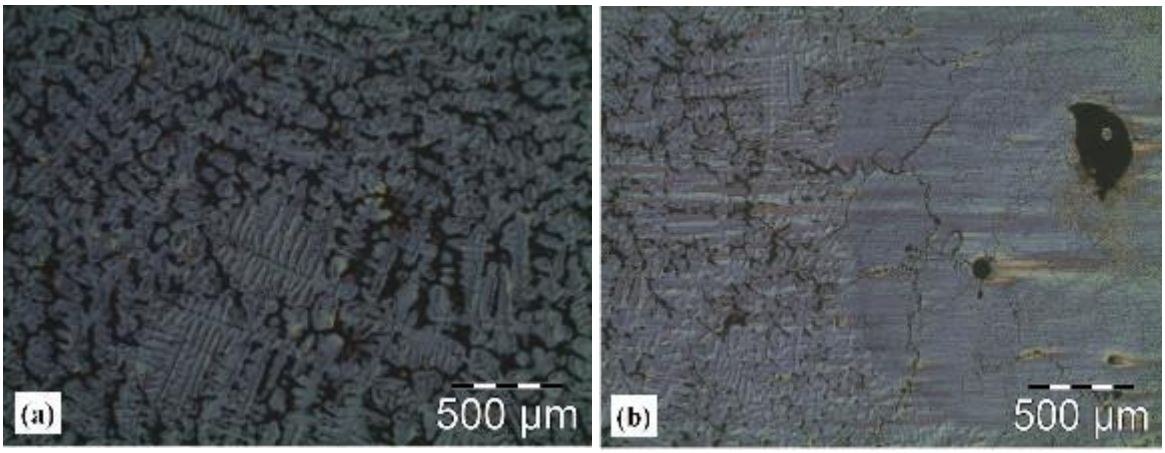

Figure 3. Base metal dendritic structure (a) and transition region between base metal and HAZ (b) of the rotor blade. 50 times increase. Electrolyte attack with 10% oxalic acid.

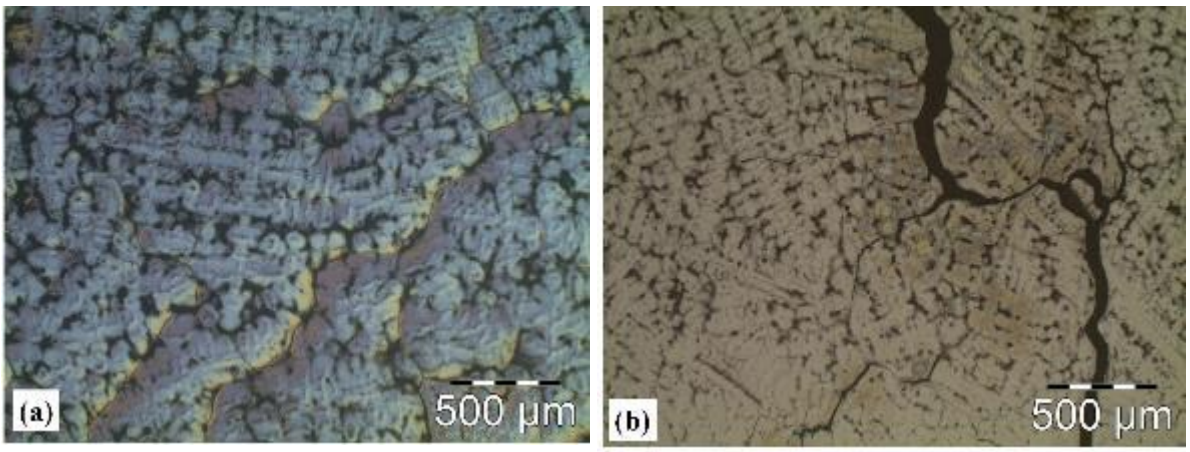

Figure 4. Dendritic structure of the base metal (a) and transition region between base metal and HAZ (b) of the rotor crown. 50 times increase. Electrolyte etching with 10% oxalic acid.

Table 1 presents hardness values in each section of the rotor samples.

Table 1. Hardness values obtained in the blade and crown samples of the Francis rotor.

Sample	Hardness (HRB)	Hardness (HB)
Blade - base metal (a)[1]	85 ± 1	164 ± 5
Blade - heat affected zone (b)[1]	101 ± 1	242 ± 3
Blade - cavitated region (b)[1]	88 ± 2	174 ± 3
Crown - base metal (c)[1]	86 ± 2	167 ± 2
Crown - heat affected zone (d)[1]	105 ± 4	251 ± 5
Crown - cavitated region (d)[1]	87 ± 1	171 ± 2

(1) measured at room temperature (25°C)

Table 2 presents the chromium and nickel content measured by the EDX analysis.

Table 2. Chemical composition of the ASTM A743 GR CF 20 stainless steel sample obtained in the EDX.

Chemical element	Percentage obtained (%)	Percentage of standard ASTM A743 (%)
Chromium (Cr)	19,02	18 - 21
Nickel (Ni)	8,32	08 - 11

4. DISCUSSION

As can be seen from the macrograph obtained from the sample of the Francis rotor shown in Figure 5, the presence of cracks and pits resulting from wear due to cavitation. According to Jiménez (2014), these cracks present on the rotor crown surfaces deplete the energy absorption capacity of stainless steel ASTM A743 GR CF20, a characteristic conferred on the hardness values obtained in cavitated regions in the blade and crown samples of the rotor. The average hardness value obtained in the cavitated region of the rotor blade was 174±3 HB while in the cavitated region of the crown it has an average hardness value of 171±2 HB, values above the recommended by the standard. According to ASTM A743 (2013) standard, the average hardness value of CF20 stainless steel in the state of delivery condition is 163 HB. The increase in hardness of the material is caused by extreme operating conditions, with complex flow and high-water velocity under the turbine, and that the increase in hardness reduces the energy absorption capacity of the material, that is, it weakens it. Due to the nature of cavitation, the result is an accelerated material removal rate. The presence of pits, cracks and craters is also related to the properties of the material.

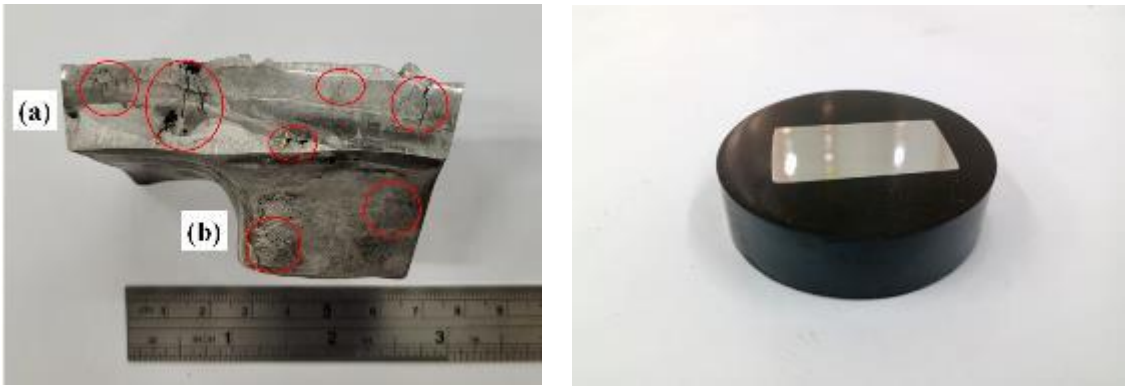

Figure 5. Macrograph of the rotor sample indicating thermally affected regions, cracks and pits due to cavitation wear in the regions of the crown (a) and blade (b). To carry out the hardness test, it was necessary to embed samples corresponding to the rotor crown and blade.

Figure 6 shows the micrographs of the crown (a) and blade (b) of the Francis rotor. It is possible to observe the sensitization present in the grain boundaries, which corresponds to intergranular corrosion, a remarkable characteristic of the recurrent failure mechanism of ASTM A743 GR CF20 stainless steel. According to Jiménez (2014), Fe-Cr-Ni alloys with 16% to 19% chromium and 6% to 22% nickel in their chemical composition, have an austenitic matrix susceptible to stress corrosion and sensitization due to precipitation. of chromium carbides in the grain boundaries, which promote the depletion of chromium in the regions adjacent to the boundaries, leading to the occurrence of intergranular corrosion.

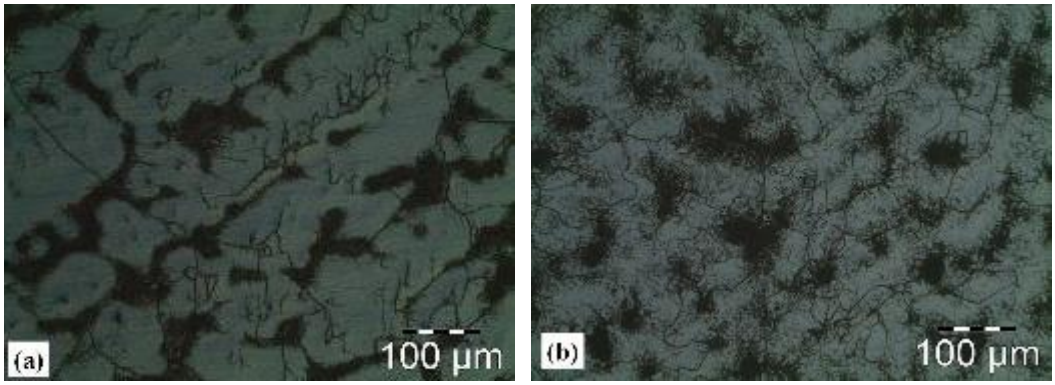

Figure 6. Micrographs of the rotor crown (a) and blade (b), showing intergranular corrosion (sensitization) in the austenitic grain boundaries. Electrolyte attack with 10% oxalic acid.

Figure 7 shows, respectively, the micrographs of the region of the crown and the blade, showing the Heat Affected Zone (HAZ), resulting from a possible solubilization of the ASTM A743 GR CF20 stainless steel alloy elements during the welding process, i.e., that is, the metal was heated to too high a temperature, obtaining the uniform austenitic phase (a, c). It is also noted in the micrograph of the rotor blade the presence of intergranular cracks resulting from the sensitization of the material in this region, which weakens the grain boundary and with the state of tensile stresses subjected especially to the blades during operation. The growth of these cracks and the formation of pits (b, d). In image (b) the presence of a perfectly spherical pitting is also observed. It is known that the crack advances perpendicular to the applied stress, so the path of the crack gives an idea of the direction of the stress in the component. It is inferred that the spherical cavity produces a stress concentration, which assists the intergranular cracking process in the material. The stresses developed in the blade are greater than in the crown, so the crack observed also has the effect of assisting cracking by the cavity and hardening of the material in cavitation. Another relevant observation is the grain size of the blade's HAZ. The size and grain is clearly larger in the HAZ of the blade, as a result of having raised the welding temperature, which caused grain growth and diffusion of Cr and C, generating sensitization in the grain boundary.

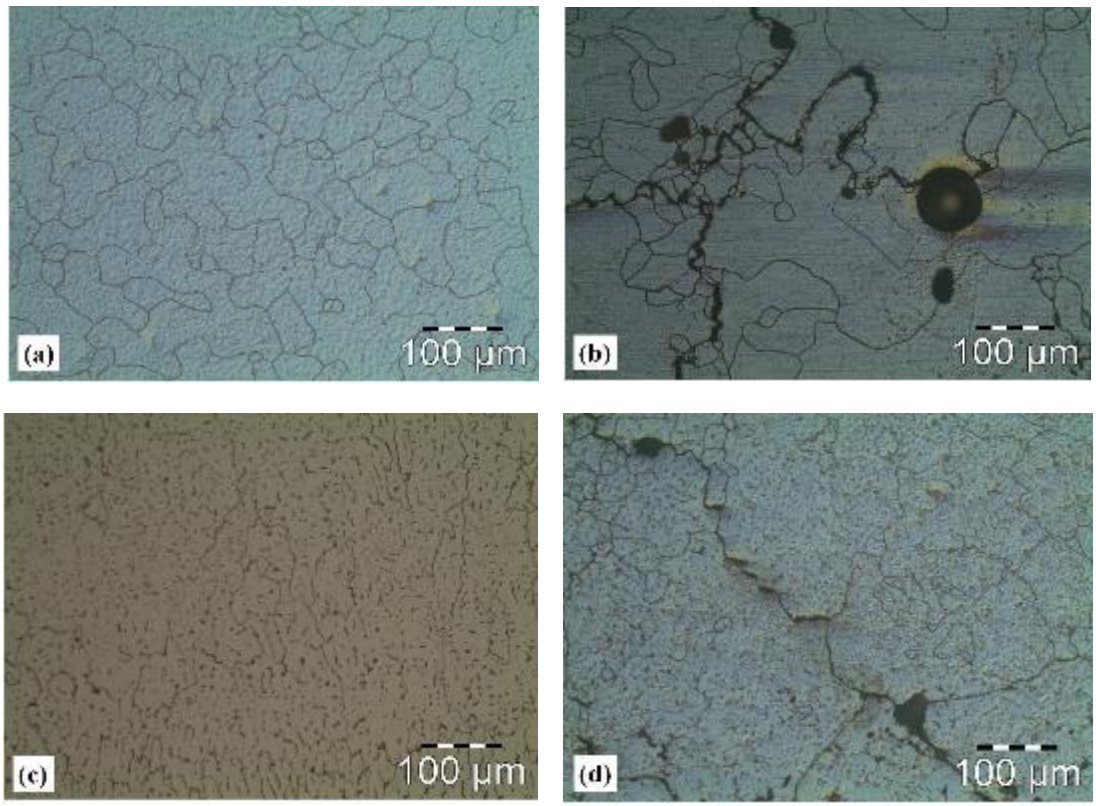

Figure 7. Micrograph of the HAZ of the blade (a), presence of intergranular cracks and pits in the austenitic matrix of the blade (b), Micrograph of the HAZ of the crown (b) and presence of intergranular cracks and pits in the austenitic matrix of the blade crown (d), Magnified 200 times. Electrolyte etching with 10% oxalic acid.

Figures 8 and 9, images taken in SEM can be seen in the HAZ region of the sample of the rotor blade with wear points on stainless steel ASTM A743 GR CF 20. It is possible to observe that the main deformation mechanisms are the pulling out of the material by micro-fracturing us from the grain boundaries and micro-reliefs-micro-reliefs formed due to the impact of the cavitation shock wave. Due to the material's low capacity for plastic deformation in this extreme operating condition, small wear points can also be observed on the surface of the grains, so that microfractures cause significant material loss, making them the dominant wear mechanism. According to Procopiak (1997), it is very common for materials such as CF20 stainless steel to present failures, caused by the propagation of intergranular cracks, due to its low capacity to absorb energy during the impact of bubbles and microjets resulting from cavitation. If cracking occurs, the material may already be weakened by local wear (which we observe with the increase in hardness) and may have crack initiators, such as stress concentrators, which appears there in the figure, or even from the center of the grain with the Chromium Carbide as initiator. This crack appears to have started at the grain boundary, or at a spherical point close to the grain boundary. This is a small cavity or inclusion in the grain. It can generate a stress concentrator that aided cracking towards the grain boundary. this being the main reason why these types of materials are less resistant to cavitation wear.

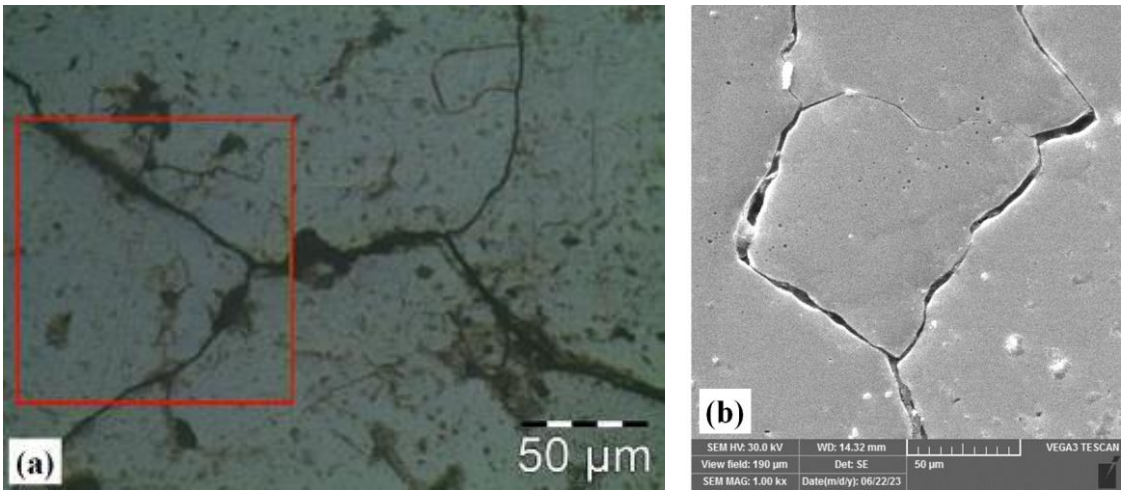

Figure 8. Micrograph of the rotor blade sample in the austenitic matrix through the Optical Microscope with intergranular cracks and pits (a) and micrograph by SEM referring to the highlighted region showing deformation on the surface of the grain and the presence of micropits (b).

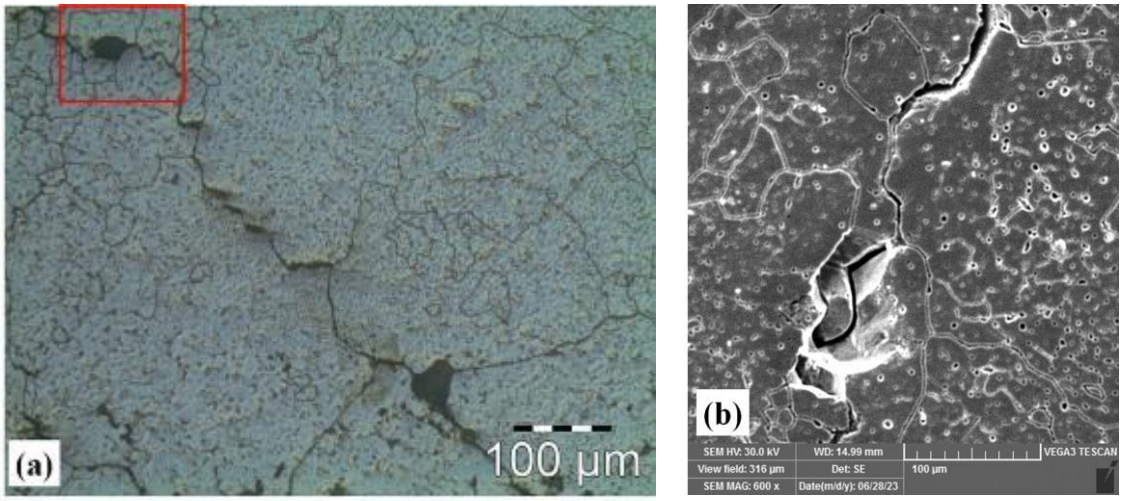

Figure 9. Micrograph of the rotor blade sample in the austenitic matrix through the Optical Microscope with intergranular cracks and pits (a) and micrograph by SEM referring to the highlighted region showing deformation on the surface of the grain and the presence of micropits (b).

The Electron Dispersion Spectroscopy (EDS) test was also carried out to evaluate the chemical composition present in the grain of the microstructure. Mass values of chemical elements compatible with the chemical composition of CF20 stainless steel (see Table 3) were obtained, in accordance with ASTM A743 (2013).

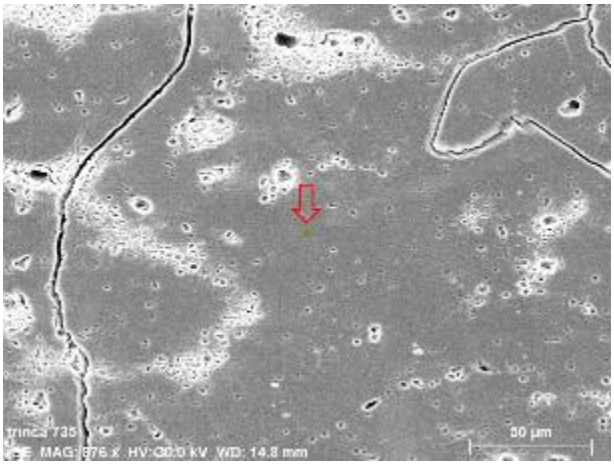

Figure 10. Analysis region of the chemical composition of the grain in the rotor blade sample.

Table 3. Chemical composition of the ASTM A743 GR CF 20 stainless steel sample obtained from the EDS.

Chemical element	Percentage obtained (%)	Percentage of standard ASTM A743 (%)
Chromium (Cr)	19,571	18 - 21
Nickel (Ni)	8,481	8 - 11
Silicon (Si)	1,224	2 (max)

5. CONCLUSIONS

The use of characterization techniques, such as microstructural analysis in an optical microscope and hardness tests, provided results consistent with the theory found in the specific literature. Based on the results obtained using these techniques, the following conclusions were reached:

- The crown and blades of the Francis rotor were significantly affected by the cavitation phenomenon. Correlating the hardness values obtained with the microstructures found in the samples, the region of the Heat Affected Zone showed excessive grain growth, due to the solubilization of the CF20 stainless steel alloy elements during the welding process, characterized by the presence of the austenitic matrix , followed by rapid cooling due to the lack of possible temperature control after welding, directly influencing the increase in hardness of the base metal, obtaining values above those allowed by ASTM A743.

- The presence of intergranular cracks and pits on the surface of the matrix grains is directly related to the phenomenon of cavitation, that is, with the increase in the hardness of the austenitic matrix, the impact of microjets and bubbles on the surface of the rotor crown influences directly on the loss of capacity to absorb energy from elastic-plastic deformation, decreasing the cavitation resistance of the base metal.

- The sensitization present in the grain boundaries of the base metal is due to the thermal welding cycle and carbon content sufficient to form Chromium Carbide in the grain boundary. Sensitization weakens the material and assists the cracking process, being a preferred site for propagation and initiation of cracking.

- The cracking observed in the grain boundary is due to the state of operational stress of the rotor and the embrittlement caused by sensitization. This, together with singularities, pullouts caused by cavitation, and other microfracture mechanisms, assist the material failure process.

6. ACKNOWLEDGMENT

The authors would like to thank the Federal Institute of Education, Science and Technology of Southeast Minas Gerais – Campus Juiz de Fora for financial support – Financing 07/2023 and Energy Company of Minas Gerais for supplying the material.

7. REFERENCES

ABNT NBR ISO 6508-1, 2019. *Metallic Materials - Rockwell Hardness Testing - Part 1: Test Method (in Portuguese).* Associação Brasileira de Normas Técnicas. Rio de Janeiro, Brasil.

ASTM A743/A743M-13a, 2013. *Standard Specification for Castings, Iron-Chromium, Iron-Chromium-Nickel, Corrosion Resistant, for General Application.* American Society of Testing and Materials. United States.

ASTM E3-11, 2017. *Standard Guide for Preparation of Metallographic Specimens.* American Society of Testing and Materials. United States.

ASTM E-140-12, 2019. *Standard Hardness Conversion Tables for Metals Relationship Among Brinell Hardness, Vickers Hardness, Rockwell Hardness, Superficial Hardness, Knoop Hardness, and Scleroscope Hardness.* American Society of Testing and Materials. United States.

Fedumenti, N., 2010. *Effect of cavitation on corrosion in stainless steels used in hydraulic turbines (in Portuguese).* Master's thesis, Graduate Program in Materials Science and Engineering, Federal University of Santa Catarina, Florianópolis, Brasil.

Hammit, F.G. and Heymann, F.J., 1975. "Liquid-erosion failures". *Failure Analysis and Prevention, Metals Handbook,* Vol. 10, p. 160-167.

Hammitt, F.G., 1979. "Cavitation erosion: The state of the art and predicting capability". *Applied Mechanics Review, ASME,* Vol. 32, pp. 665-675.

Horta, C.A., Gonçalves, C., Calainho, J.A.L. and Lomônaco, F.G., 1999. *Cavitation in francis and kaplan type hydraulic turbines in Brazil* (in Portuguese), Instituto de Pesquisas Energéticas e Nucleares, São Paulo, https://www.ipen.br/biblioteca/cd/conem/2000/OC8712.pdf. Accessed 19 Jun 2023.

Jiménez, L.BV., 2014. *Study of the micromechanisms of cavitation damage in UNS S 31803 stainless steel with high nitrogen content with and without work hardening (in Portuguese).* Master's thesis, Graduate Program in Science, University of São Paulo, São Paulo, Brasil.

Marinho, F.C., 2015. *Study of a francis turbine. Reliability-centric maintenance and abrasion analysis (in Portuguese).* Graduation project in mechanical engineering, Pontifical Catholic University of Rio de Janeiro, Rio de Janeiro, Brasil.

Procopiak, L.A.J., 1997. *Cavitation resistance of three welded coatings (in Portuguese).* Master's thesis, Graduate Program in Mechanical Engineering, University of Santa Catarina, Florianópolis, Brasil.

Richman, R.H., 1995. "Deformation-induced martensite and resistance to cavitation erosion". *Journal de Physique IV,* Vol. 5, pp. C8-1193-1198.

Scheweitzer, P.A., 1996. *Corrosion engineering handbook.* Marcel Dekker, Inc. Publisher, New York.

Xiaojun, Z., 2002. *Effect of surface modification processes on cavitation erosion resistance (in Portuguese).* Doctoral thesis, Graduate Program in Materials Science, Federal University of Paraná, Curitiba, Brasil.

8. RESPONSIBILITY NOTICE

The authors are the only responsible for the printed material included in this paper.